Characterization of TiO2 NPs in Radish (Raphanus sativus L.) by Single-Particle ICP-QQQ-MS

Justyna Wojcieszek, Javier Jiménez-Lamana, Lena Ruzik, Monika Asztemborska, Maciej Jarosz, Joanna Szpunar

frontiers in Environmental Science

ORIGINAL RESEARCH
published: 28 July 2020
doi: 10.3389/fenvs.2020.00100

Characterization of TiO_2 NPs in Radish (*Raphanus sativus* L.) by Single-Particle ICP-QQQ-MS

Justyna Wojcieszek[1], Javier Jiménez-Lamana[2], Lena Ruzik[1], Monika Asztemborska[3], Maciej Jarosz[1] and Joanna Szpunar[2]*

[1] Chair of Analytical Chemistry, Faculty of Chemistry, Warsaw University of Technology, Warsaw, Poland, [2] Universite de Pau et des Pays de l'Adour, E2S, UPPA, CNRS, IPREM UMR 5254, Pau, France, [3] Isotopic Laboratory, Faculty of Biology, University of Warsaw, Warsaw, Poland

Titanium dioxide nanoparticles (TiO_2 NPs) are increasingly used in a wide range of consumer products and industrial applications, causing their presence in the environment, where they can interact with plants including edible ones. In addition, the released TiO_2 NPs can undergo chemical and physical transformations, which may influence their potential toxicity. However, the study of TiO_2 NPs in environmental samples by the technique offering the highest sensitivity, ICP-MS, is hampered by the presence of some elements (such as, e.g., Ca abundant in plant tissues) that cause polyatomic and/or isobaric interferences. This study proposed, for the first time, the use of a triple-quadrupole ICP operating in tandem mass spectrometry and single-particle mode (SP-ICP-QQQ-MS) to study the uptake, translocation, and possible transformations of TiO_2 NPs with two different nominal sizes in a model plant (*Raphanus sativus* L.). A careful optimization of the reaction cell conditions (O_2 and H_2 gas flows) allowed the reduction in background level and resulted in a significant increase in the sensitivity of the analysis, bringing size detection limits for TiO_2 NPs down to 15 nm in ultrapure water and to 21 nm in a matrix containing 50 mg L^{-1} of Ca. In addition, an enzymatic digestion procedure was applied in order to extract intact nanoparticles from the tissues of plants treated with TiO_2 NPs, followed by size characterization by SP-ICP-MS. The size distributions obtained in roots treated with TiO_2 NPs suggested a preferential uptake of smaller nanoparticles. Results also revealed that the majority of TiO_2 NPs were retained in roots. Additionally, no significant dissolution was observed, as well as no differences for nanoparticles found in roots and leaves, proving that radish is able to translocate intact TiO_2 NPs up to aboveground organs.

Keywords: titanium dioxide nanoparticles, model plant, tandem mass spectrometry, single particle ICP-MS, uptake, translocation, size characterization

OPEN ACCESS

Edited by:
Denise M. Mitrano, Swiss Federal Institute of Aquatic Science and Technology, Switzerland

Reviewed by:
Nathaniel Clark, University of Plymouth, United Kingdom
Geert Cornelis, Swedish University of Agricultural Sciences, Sweden
Manuel David Montaño, Western Washington University, United States

****Correspondence:***
Javier Jiménez-Lamana
j.jimenez-lamana@univ-pau.fr

Specialty section:
This article was submitted to Biogeochemical Dynamics, a section of the journal Frontiers in Environmental Science

Received: *31 March 2020*
Accepted: *09 June 2020*
Published: *28 July 2020*

Citation:
Wojcieszek J, Jiménez-Lamana J, Ruzik L, Asztemborska M, Jarosz M and Szpunar J (2020) Characterization of TiO_2 NPs in Radish (Raphanus sativus L.) by Single-Particle ICP-QQQ-MS. Front. Environ. Sci. 8:100. doi: 10.3389/fenvs.2020.00100

INTRODUCTION

With the fast development of nanotechnology over the past decade, there are more and more applications of nanomaterials in daily life, e.g., in many commercial and industrial products, medicine, electronics, and energy sectors. Especially, metal and metal-oxide nanoparticles have been widely applied in different fields due to their unique physical and chemical properties. Among

them, titanium dioxide nanoparticles (TiO_2 NPs) are one of the most widely applied nanoparticles (Capaldi Arruda et al., 2015; Shah et al., 2017). TiO_2 NPs occur in three different crystallographic forms: anatase and rutile (tetragonal) and, more rarely, brookite (orthorhombic). Among those three major polymorphs, anatase is extensively applied in commercial products due to its higher activity comparing to other forms, although rutile is the more stable form (Chen and Mao, 2007; Zhang et al., 2015). Additionally, there are no commercial TiO_2 NPs products in the brookite phase (Tan et al., 2018). Titanium is a common metal in soil that occurs in naturally occurring nano-sized particles, such as clays. It is important to mention that TiO_2 found in soil is known to be rather non-toxic to most organisms. TiO_2 NPs are being used for many products such as plastics, paints, surface coatings, medical devices, cosmetics, and nanofertilizers (Hong et al., 2017). They are applied as food additives or in nutritional supplements, and therefore, oral exposure to TiO_2 NPs may happen through the consumption of such products (Shakeel et al., 2016). In the field of nanomedicine, an intravenous injection can deliver TiO_2 NP carriers directly into the human body (Shakeel et al., 2016). Because of their UV light-resistant properties, TiO_2 NPs are also commonly used in sunscreens or toothpaste (Vidmar et al., 2017). In general, TiO_2 NPs account for about 70% of the total production volume of pigments worldwide and are in the top five NPs used in consumer products (Jafarizadeh-Malmiri et al., 2019; Dar et al., 2020).

The wide applications of TiO_2 NPs have raised serious concerns regarding their potential threat to the environment, as during their whole life cycle, TiO_2 NPs may be released into the air, soil, and/or water, affecting all components of the environment, including plants, which are directly exposed to these emerging contaminants (Oliver et al., 2015; Tan et al., 2018). It has been reported that the emission of TiO_2 NPs represents more than one-fourth of the estimated mass flow of engineered nanoparticles (ENPs) in a worldwide range (Keller and Lazareva, 2013). By the year 2025, the estimated global production of TiO_2 NPs would be 1000 tons, and once they persist for a long time in the environment, the chances of exposure to plants will increase and therefore a better understanding of the possible toxicity of TiO_2 NPs is important in assessing environmental risks (Du et al., 2019). In addition, it has to be taken into account that the potential toxicity of released NPs may be influenced by the different transformations they can undergo, which are still not well understood. If TiO_2 NPs enter the environment, they become bioavailable to plants and hence their impact on edible plants and food safety needs to be further investigated (Capaldi Arruda et al., 2015; Dan et al., 2015; Reddy et al., 2016). However, it is important to remember that the presence of Ti-containing clays could disturb the investigation of plants exposed in real soil (i.e., not hydroponically) from the ecotoxicological point of view. During the studies, the clays should be removed from the plant, to avoid contamination of the sample since they would not be distinguishable from TiO_2 using single-element SP-ICP-MS.

The study of the interactions between TiO_2 NPs and plants has been addressed through different analytical techniques, such as microscopy (electron, optical, fluorescence, or confocal), mass spectrometry, UV-Vis, and FT-IR spectroscopy and ICP-based and μX-ray techniques (Tan et al., 2018). Electron microscopy (scanning – SEM and transmission – TEM) and ICP-OES/MS have been widely used due to their capability to determine the size and shape of NPs in plant cells and their high sensitivity, respectively (Kole et al., 2016). For instance, the accumulation of TiO_2 NPs in roots and leaves of rice (*Oryza sativa*) and their adsorption on the surface of the roots of lettuce were shown by using TEM, SEM, and ICP-OES/MS techniques (Cai et al., 2017; Deng et al., 2017). However, the low resolution of electron microscopy or the complicated sample preparation may bring some difficulties during the analysis (Larue et al., 2014; Tan et al., 2018). Synchrotron-based techniques can provide higher resolutions than microscopy, although they require high concentrations of NPs (Castillo-Michel et al., 2017). By using μX-ray fluorescence (μ-XRF) and μX-ray absorption near edge structure (μ-XANES), it has been shown that TiO_2 NPs can be translocated from roots to stems (in lettuce – *Lactuca sativa*) (Larue et al., 2016), leaves (Servin et al., 2012), and even fruits (in cucumber – *Cucumis sativus*) (Servin et al., 2013). TEM and μ-XRF have shown the presence of TiO_2 NPs in nuclei and vacuoles of *Arabidopsis thaliana* roots and leaf stomata (Kurepa et al., 2010). It should be also highlighted that plant cultivation with TiO_2 NPs influences accumulation of other elements. For example, the increasing content of P, Ca, Mg, and Zn was determined in roots, shoots, and grains of rice (Du et al., 2017; Zahra et al., 2017), whereas an enhanced accumulation of Fe in roots (Burke et al., 2015) was shown in the case of soybean. On the other hand, the differences in the physicochemical properties of TiO_2 NPs such as their size, aggregation, surface area, coating, and crystal structure have a huge influence on the interactions of NPs with living organisms like plants, inducing different toxicities (Du et al., 2019). In this context, size characterization and monitoring of different processes that nanoparticles may undergo (agglomeration, dissolution) have to be monitored throughout the whole interaction with plants: contact with the growth medium, uptake by roots, and translocation to aboveground organs. Additionally, the investigation and study at environmentally relevant concentrations require the use of the highest-sensitivity techniques.

Single-particle inductively coupled plasma mass spectrometry (SP-ICP-MS) is a well-established technique used for the detection, characterization, and quantification of engineered nanoparticles in environmental samples (Laborda et al., 2016). SP-ICP-MS is able to provide information about particle size, particle concentration, and dissolved element concentration as well as to monitor possible transformation processes like agglomeration or dissolution. These metrics cannot be routinely measured with the abovementioned techniques. However, the analysis of TiO_2 NPs in environmental samples using conventional single-quadrupole instruments (ICP-Q-MS) presents some challenges. In fact, the determination of Ti in plant tissues can be hindered by the presence of Ca, since the most abundant isotope of Ti, ^{48}Ti (73.7% abundance), suffers an isobaric interference from one of the isotopes of Ca (^{48}Ca). Therefore, studies using single-quadrupole ICP-MS are compelled to monitor less interfered Ti isotopes, such as ^{47}Ti and ^{49}Ti, with 7.4% and 5.4% abundances, respectively, rendering

the detection of smaller TiO_2 NPs more difficult due to a lower sensitivity of ICP-MS. These limitations can be overcome by using triple-quadrupole ICP-MS (ICP-QQQ-MS), allowing for controlled interference removal by introducing a reaction gas, which interacts with the interfering ions. It leads to higher sensitivity thanks to the monitoring of the most abundant ^{48}Ti isotope (73.7% abundance), which suffers an isobaric interference from ^{48}Ca, and gives a possibility of an effective characterization of low-size TiO_2 NPs in biological and environmental samples.

In the context of the widespread production and distribution of TiO_2 NPs in different fields and the possible risk regarding their release into the environment, the main purpose of this work was to study the uptake, translocation, and possible transformations of TiO_2 NPs in the model plant, radish (*Raphanus sativus L.*), a popular vegetable consumed all over the world whose edible part is in direct contact with the soil where contamination may take place. After a careful optimization of reaction cell conditions, the fate of two TiO_2 NPs suspensions with different nominal sizes in radish was studied by means of tandem ICP-MS in single-particle mode (SP-ICP-QQQ-MS). The use of tandem mass spectrometry allowed the monitoring of ^{48}Ti in plant tissues, hence improving the sensitivity and size detection limit. To the best of our knowledge, this is the first application of triple-quadrupole ICP in the study of the interactions of TiO_2 NPs with edible plants in single-particle ICP-MS mode.

MATERIALS AND METHODS

Samples and Reagents

Seeds of radish (*Raphanus sativus* L.) were purchased from Vilmorin Garden (Komorniki, Poland). Analytical- or biological reagent-grade chemicals and LC-MS-grade solvents were purchased from Sigma-Aldrich (St. Louis, MO, United States), unless stated otherwise. Ultrapure water (18 MΩ cm) obtained with a Milli-Q system (Millipore, Guyancourt, France) was used throughout this work. The nitric acid of purity for trace metal analysis was purchased from Fluka (Buchs, Switzerland). An ionic standard solution of 1000 mg L^{-1} titanium was purchased from Agilent Technologies (Tokyo, Japan). Macerozyme R-10 enzyme (pectinase from *Rhizopus* sp., Sigma-Aldrich), a multicomponent enzyme mixture containing cellulase (0.1 unit per mg), hemicellulase (0.25 unit per mg), and pectinase (0.5 unit per mg), was used to digest plant tissues for TiO_2 NP extraction.

Powder of TiO_2 NPs in rutile form with nominal sizes of 30 and 100 nm was purchased from US Research Nanomaterials, Inc. (Houston, TX, United States). Stock suspensions of TiO_2 NPs (500 mg L^{-1}) were prepared by dispersion of NP powder (25 mg) in ultrapure water (50 mL). These stock suspensions will be referred to as suspension A (nominal diameter: 30 nm) and suspension B (nominal diameter: 100 nm) throughout the rest of the manuscript. Diluted suspensions of TiO_2 NPs were prepared daily in ultrapure water by accurately weighing aliquots of the stock suspensions after 1-min sonication. Before each analysis, the suspensions were bath sonicated for approximately 1 min. A gold nanoparticle (AuNPs) standard with a nominal diameter of 50 nm (BBI Solutions, Cardiff, United Kingdom) was used for the determination of transport efficiency. All suspensions of nanoparticles were stored in darkness at 4°C and sonicated directly before SP-ICP-MS analysis.

Instrumentation

Homogenization of the plant tissues was performed by a KIMBLE Dounce tissue grinder set of 7 mL (Sigma-Aldrich). Incubation of samples was performed in a Memmert water bath (Memmert, Schwabach, Germany). A Bandelin DT 52 H ultrasonic bath (BANDELIN Electronic, Berlin, Germany) was used for sonication of nanoparticle suspensions and enzymatic extraction before SP-ICP-MS analysis.

Single-Particle ICP-MS Method

Characterization of TiO_2 NPs was carried out using an Agilent 8900 ICP-QQQ-MS equipped with a Single Nanoparticle Application Module. The default instrumental and data acquisition parameters are listed in **Table 1**. The position of the torch and nebulizer gas flow was adjusted each day of work with special emphasis to decrease the level of CeO/Ce below 0.2% with the aim to minimize the risk of polyatomic interferences caused by oxide formation. The working conditions of ICP-MS were optimized daily using a 1-μg L^{-1} solution of $^{7}Li^{+}$, $^{89}Y^{+}$, and $^{205}Tl^{+}$ in 2% (v/v) HNO_3. During analysis, ^{48}Ti with a natural abundance of about 73.7% was monitored. The reaction gas containing O_2 and H_2 was used in order to resolve the spectral interferences on ^{48}Ti. The use of O_2 as reaction cell gas allows the analysis of ^{48}Ti by monitoring the oxide ion at m/z + 16 u, which means that the ICP-QQQ-MS instrument worked in "mass-shift" mode during this study. Therefore, the first quadrupole was set to m/z 48 (the precursor ^{48}Ti ion) and the second quadrupole was set to m/z 64 (the target product ion $^{48}Ti^{16}O$). O_2 promoted the formation of the $^{48}Ti^{16}O^{+}$ product ion, and H_2 helped with the formation of $^{48}Ca^{16}O^{1}H^{+}$, avoiding interference on $^{48}Ti^{16}O^{+}$ by $^{48}Ca^{16}O^{+}$. In addition, working in mass-shifted mode allows one to avoid any potential isobaric interference at m/z 64 like ^{64}Zn, since these ions are filtered by the first quadrupole. SP-ICP-MS analyses

TABLE 1 | Default instrumental and data acquisition parameters for SP-ICP-MS.

Instrumental parameters	
RF power	1550 W
Plasma, auxiliary, and nebulizer gas flow	15.0, 0.9, and 1.15 L min^{-1}
H_2 gas flow	8 mL min^{-1}
O_2 gas flow	10%
Cones	Skimmer – Ni, sampler – Ni
Sample uptake rate	0.35 mL min^{-1}
Data acquisition parameters	
Dwell time	100 μs
Readings per replicate	600000
Total acquisition time	60 s
Analyte	Ti
Mass (amu)	48 (48 → 64)
Density	4.61 g cm^{-3}
Mass fraction	0.6

were performed in time-resolved analysis (TRA) mode using a dwell time of 100 μs, with a total time of data acquisition of 60 s. A AuNPs standard with a nominal diameter of 50 nm was used for the determination of transport efficiency, which was calculated by the particle size method described by Pace et al. (2011). The sample flow rate was calculated daily by measuring the mass of water taken up by the peristaltic pump for 2 min (this operation was repeated three times). Under the experimental conditions used in this work, the transport efficiency at a sample flow rate of 0.35 mL min^{-1} was 6%. After each sample analysis, the software automatically processed the raw data and generated the particle size, particle concentration, size distribution, and information about the concentration of dissolved metal. The dwell time is a critical parameter in single-particle detection mode. Working with microsecond dwell times allows the recording of particle events as resolved transient signals, improving hence the resolution and working range. In this work, the discrimination between dissolved signal and nanoparticle signal was done in the basis of threshold (I_{thresh}) determined as $I_{thresh} = I_b + 5\sigma_b$, where I_b is the intensity of the baseline and σ_b the standard deviation of the baseline of each sample. A criterion of $5\sigma b$ was recently considered as a good compromise (Laborda et al., 2019).

Scanning Electron Microscopy Analysis

Electron-microscopy images were taken with the use of a Hitachi SU8230 ultra-high-resolution field-emission scanning electron microscope (Hitachi High-Technologies Corporation) using secondary electron detectors (SE) at a 30.0-kV accelerating voltage. Images were taken with the use of gold TEM grids coated with a Lacey carbon film, which were immersed in samples in the form of DI water suspensions and dried prior to observation. Magnifications used were in the range of ×100 000–350 000.

Procedures

Plant Cultivation

Portions of radish seeds (ca. 1 g) were germinated in distilled water in darkness for 3 days, and then the seedlings were transferred to 350-mL containers with a Knop nutrient solution (the composition is shown in **Supplementary Table 1**) and placed in a growth chamber. After 4 days, the TiO_2 NP suspension of different sizes (30 and 100 nm) was added separately to three different containers with the medium at a titanium concentration of 5 mg L^{-1}. As a control variant, plants were left in the nutrient solution without the addition of titanium. Cultivation was carried out for the next 7 days in a growth chamber. Each variant of the cultivation was performed in three replicates. After cultivation, the plants were harvested and the roots were gently rinsed with deionized water. The plants were divided into roots and aboveground organs (leaves plus stems) and lyophilized. Dried plant material was ground in a mortar before further analysis.

Enzymatic Digestion Method

After the cultivation of radish, plant tissues were digested enzymatically as reported in previous works (Jiménez-Lamana et al., 2016; Wojcieszek et al., 2019), with small modifications, as it was necessary to change the way of sample homogenization. Therefore, grounded samples of leaves together with stems and roots (0.020 g) were homogenized for 15 min with 7 mL of 2 mM citrate buffer (pH 4.5; adjusted with citric acid) by using a tissue grinder set. The ultrasonic probe used in previous works could not be used due to the fact that its composition contains titanium and a significant amount of Ti was detected even in blanks. After the end of homogenization, 1.5 mL of Macerozyme R-10 solution (0.01 g of enzyme powder for roots and 0.04 g of enzyme powder for leaves plus stems, dissolved in 1.5 mL of ultrapure water) was added to samples, and the samples were next shaken at 37°C for 24 h in a water bath with continuous shaking. After digestion, the samples were settled down for approximately 60 min and the obtained supernatants were analyzed by SP-ICP-MS. Filtration studies were performed by using syringe filters of 0.45 and 1.0 μm pore size with PTFE and PES membrane purchased from VWR (Gdańsk, Poland).

RESULTS AND DISCUSSION

Development and Optimization of an Analytical Method Based on SP-ICP-QQQ-MS for the Characterization of TiO_2 NPs in Plant Tissues

Optimization of H_2 and O_2 Gas Flows

When working on SP-ICP-MS, special attention should be paid to the size limit of detection. This limit is dependent on the response of the instrument toward the isotope monitored and on the background signal, with the latter critically affected by isobaric and polyatomic interferences. The higher the background signal, the lower the capability of detecting small nanoparticles and hence the higher the size limit of detection. This is especially relevant for the determination of TiO_2 NPs in real samples like plant tissues, since the most abundant ^{48}Ti isotope (73.7% abundance) suffers an isobaric interference from one of the isotopes of Ca (^{48}Ca), which is an essential plant nutrient (White and Broadley, 2003). In order to overcome this problem, ^{48}Ti was measured in mass-shifted mode by using a mixed O_2/H_2 cell gas.

Prior to the analysis of the plant samples, the O_2/H_2 cell gas was optimized in terms of flow of both gases. To do that, three different matrices were analyzed: ultrapure water, 1 mg L^{-1} Ca, and 50 mg L^{-1} Ca. The three solutions were analyzed by means of single-particle ICP-MS according to the conditions shown in **Table 1** and with varying flows of H_2 and O_2. For each condition tested (i.e., different O_2 and H_2 flows), the response of the instrument toward Ti was obtained, in terms of per ppb of Ti, by analyzing a solution of 0.5 ppb. Subsequently, the three matrices were analyzed and the corresponding signal provided by the software was treated mathematically in order to obtain the associated noise (calculated as δ), and hence the signal-to-noise ratio was obtained.

Figure 1A shows the signal-to-noise ratios obtained by using different H_2 flows (from 5 to 9 mL min^{-1}) for the analysis of the three different matrices. The presence of Ca at relatively low concentrations (1 mg L^{-1}) did not have a significant effect since

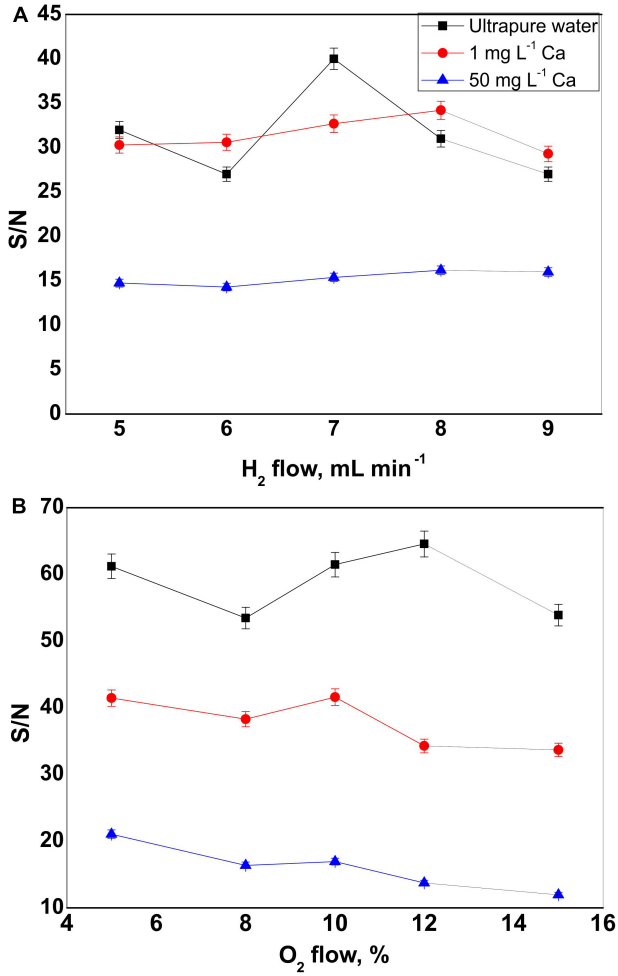

FIGURE 1 | Signal-to-noise ratio obtained for three different matrices: ultrapure water (black line, squares), 1 mg L^{-1} Ca (red line, circles), and 50 mg L^{-1} Ca (blue line, triangles) at different **(A)** hydrogen gas flows, and **(B)** oxygen gas percentages. Error bars represent the standard deviation of the measurement.

signal-to-noise ratios obtained were similar to those obtained for ultrapure water for the different flows studied. However, this ratio dropped dramatically (around 50%) when the Ca concentration increased up to 50 mg L^{-1}. The best ratios were obtained with H_2 flows of 7 and 8 mL min^{-1} for ultrapure water and calcium-containing matrices, respectively. Since a significant amount of Ca is expected in plant tissues [up to 0.1–5% of dry weight (Thor, 2019)], an H_2 flow of 8 mL min^{-1} was retained for the rest of the experiment.

The O_2 flow was optimized in a similar way. O_2 gas at percentages of 5, 8, 10, 12, and 15 was tested, and the corresponding signal-to-noise ratios were obtained for the three mentioned matrices. As it is shown in **Figure 1B**, the ratio decreased significantly when analyzing titanium in a matrix highly charged in calcium. On the other hand, the best results for both calcium-containing matrices were obtained when working at 5 and 10% of O_2. In order to promote a more significant formation of $^{48}Ti^{16}O^+$ from $^{48}Ti^+$ in the first quadrupole, the higher O_2 flow (10%) was chosen for the rest of the study.

Size Detection Limit

The attainable size detection limit (LOD_{size}) is directly affected by the standard deviation (σ_B) of the intensity corresponding to the background and/or to the dissolved species. By applying a 3σ criterion (Laborda et al., 2014), the size detection limit can be calculated through the following equation:

$$LOD_{size} = \left(\frac{18\sigma_B}{\pi \rho X_{NP} K_{ICPMS} K_M} \right)^{\frac{1}{3}} \quad (1)$$

where ρ is the density of the particles (g cm^{-3}), X_{NP} is the mass fraction of the element in the particle, K_{ICPMS} is the detection efficiency (ratio of the number of ions detected vs. the number of atoms of the isotope introduced into the ICP), and K_M (= AN_{Av}/M_M) is related with the contribution from the element measured (A is the atomic abundance of the isotope considered; N_{Av}, the Avogadro number; M_M, the atomic mass of the element). K_{ICPMS} can be deduced from the equation that relates the signal R (ions counted per time unit) and the mass concentration of a solution of the analyte, C^M (Laborda et al., 2014):

$$R = K_{intr} K_{ICPMS} K_M C^M \quad (2)$$

where K_{intr} (= η_{neb} Q_{sam}) can be estimated through the transport efficiency and the sample uptake rate (η_{neb} and Q_{sam}, respectively, whose values are detailed in "Materials and Methods"). Therefore, by knowing K_{intr} and K_M and by analyzing a dissolved titanium standard, K_{ICPMS} can be determined. σ_B is estimated as the experimental standard deviation of the baseline of the sample (Laborda et al., 2019). Since in this work the signal baseline in samples is mainly caused by the presence of Ca, σ_B was calculated from three different Ca background levels.

Size detection limits, calculated for ^{48}Ti, of 15, 16, and 20 nm, were obtained for ultrapure water, 1 mg L^{-1} Ca, and 50 mg L^{-1} Ca matrices, respectively. As it can be observed, an increase in the Ca concentration in the matrix implies an increase in the baseline and, inevitably, of its noise, which leads to an increase in σ_B and hence in the LOD_{size}. In any case, the use of a triple-quadruple ICP tandem mass spectrometry operating in mass-shift mode allowed the use of the most abundant isotope ^{48}Ti, through the monitoring of its oxide $^{48}Ti^{16}O^+$, achieving size detection limits of 15 nm in ultrapure water and 20 nm in a matrix highly charged in calcium. This LOD_{size} represents a gain of a factor of 5 with respect to those attainable by monitoring less abundant Ti isotopes by single-quadrupole ICP-MS (Lee et al., 2014). In addition, the use of an O_2/H_2 reaction cell resulted in better size detection limits than those reported by using other reaction gases: 64 nm in ultrapure water and 101 nm in 50 mg L^{-1} Ca were achieved with a mixture of ammonia and helium (Tharaud et al., 2017). In comparison with studies performed by high-resolution (HR) ICP-MS (Tharaud et al., 2017), the current study presented a slightly higher LOD_{size} in ultrapure water (15 nm vs. 10 nm by HR-ICP-MS) but a significant improvement when analyzing TiO_2 NPs in a matrix containing 50 mg L^{-1} of Ca (21 nm vs. 37 nm by HR-ICP-MS). Finally, the size

detection limits obtained here by single-particle QQQ-ICP-MS in MS/MS mode were at similar levels than those reported by using double-focusing magnetic sector field ICP-MS (ICP-SF-MS): 19.2 nm for samples injected as a wet aerosol (Hadioui et al., 2019) and 20 nm for TiO_2 NPs the snow and rain waters (Azimzada et al., 2020).

Characterization of TiO_2 NP Suspensions

TiO_2 NP commercial suspensions with two different nominal sizes were analyzed by SP-ICP-MS with the optimized cell gas conditions. The corresponding size distributions are shown in **Figures 2A,B**. For both suspensions, highly polydisperse distributions and nanoparticles of bigger diameters than the nominal ones provided by the manufacturer were obtained. Nanoparticles with sizes ranging from 100 to 400 nm were observed for both suspensions analyzed. In addition, median diameters of 180 ± 13 and 220 ± 10 nm were obtained for commercial suspensions A and B, with nominal sizes of 30 and 100 nm, respectively (**Table 2**). In order to discard any artifact during SP-ICP-MS measurements and/or calculations, both commercial suspensions were analyzed by SEM. The images (**Supplementary Figure 1**) reflected the high polydispersity of both suspensions, with sizes up to 400 nm and only a few with sizes below 100 nm, which is in good agreement with the results obtained by SP-ICP-MS. On the other hand, images show a certain degree of particle agglomeration. Even though nanoparticle suspensions are analyzed by SP-ICP-MS at a very low concentration and after bath sonication, the occurrence of some agglomerates is still likely to happen, as it will be discussed in detail below. Images obtained by SEM also showed several non-spherical nanoparticles. It is important to emphasize this information since SP-ICP-MS calculations that allow to get the size distribution of nanoparticles are based on the assumption that nanoparticles are spherical. Therefore, this may inevitably lead to a certain degree of inaccuracy on the size distributions obtained for both suspensions by SP-ICP-MS. However, the purpose of this study, i.e., the uptake of TiO_2 NPs by radish and the investigation of the possible transformation of nanoparticles, was not hampered by this fact.

Influence of Enzymatic Digestion

In order to check if the enzymatic procedure affects the size distribution of the TiO_2 NPs, suspensions of both commercial TiO_2 NPs were prepared at a concentration of titanium of 5 mg L^{-1}, without the presence of a plant matrix, and treated with the same conditions of enzymatic digestion as later applied for plant tissues. After incubation and analysis, the obtained results showed that the size distributions obtained for enzyme-treated TiO_2 NPs were in good agreement with the size distributions obtained for TiO_2 NPs stock suspension freshly prepared, regardless of the analyzed size of NPs (**Figures 2C,D**). It is worth mentioning that in the case of suspension B, the presence of nanoparticles with sizes around 20 nm and slightly above after the enzymatic digestion is more important than in the case of the size distribution obtained for the stock suspension. This fact would be explained by redispersion of smaller nanoparticles after enzymolysis corroborating the hypothesis of the presence of small agglomerates in the stock suspension. In any case, the integrity of TiO_2 NPs is not affected by the enzyme used in the digestion procedure. Therefore, it can be concluded that the Macerozyme R-10 enzyme used for enzymatic digestion was suitable for extracting intact TiO_2 NPs from plant tissues.

Influence of Filtration on the Size Characterization and Quantification of Extracted Nanoparticles

Filtration and ultrafiltration are membrane transport processes, widely used to separate solid particles, colloids, or macromolecules from fluids. Before analysis by ICP-MS, filtration is often used in order to prevent the introduction of particulate matter into the system, which may result in blocking of the nebulizer or in the contamination of the inner parts of the instrument. One of the advantages of membrane techniques is the possibility of separation of different species without using separating agents, decreasing then the probability of contamination. However, membrane filtration may be distorted by some physicochemical artifacts such as aggregation of compounds of any size at the membrane surface (Fedotov et al., 2011; Vidmar et al., 2017). In this sense, the influence of filtration on the number of nanoparticles detected during SP-ICP-MS analysis was investigated before analysis of plant samples. Both TiO_2 NP suspensions were filtered through 0.45-μm filters with PTFE membrane and analyzed by SP-ICP-MS. The time scans obtained (**Supplementary Figure 2**) showed that only a small part of nanoparticles was detected in the recovered filtrates: only 15% and 3% of nanoparticles were observed after filtration TiO_2 NP suspensions A and B, respectively (**Table 3**). These phenomena can be explained by agglomeration and/or adsorption of nanoparticles on the membrane surface and pore walls. Moreover, the size distributions of filtered nanoparticle suspensions were obtained and the corresponding median diameters determined and compared with stock suspension. As it is shown in **Table 3**, the nanoparticles subjected to filtration through 0.45-μm filters presented median diameters between 60 and 70 nm lower, suggesting that bigger nanoparticles are more prone to be retained in filters. These results are contradictory with a previous study showing that TiO_2 NPs were not adsorbed on 0.45-μm syringe filters, although the nature of the membrane used was not mentioned (Vidmar et al., 2017). In order to check whether the problem with low efficiency of TiO_2 NP filtration is caused by pore size or membrane type of the filter used, two additional filters (PTFE and PES membrane with pore size of 1.0 μm) were also checked in the same way as described above. However, no significant improvement of results was observed compared to those obtained after the use of 0.45-μm filters: most of NPs still retained on the membrane surface. It can lead to the conclusion that TiO_2 NPs are adsorbed on syringe filters regardless of pore size (at least up to 1.0 μm) or membrane used. As a result, no filtration of plant samples was performed. After incubation, samples were allowed to settle down by gravity for 1 h, and the upper part of the suspension was taken for further analysis, avoiding the pipetting of the solid plant matrix. Each sample was subjected to enzymatic digestion by triplicate and good

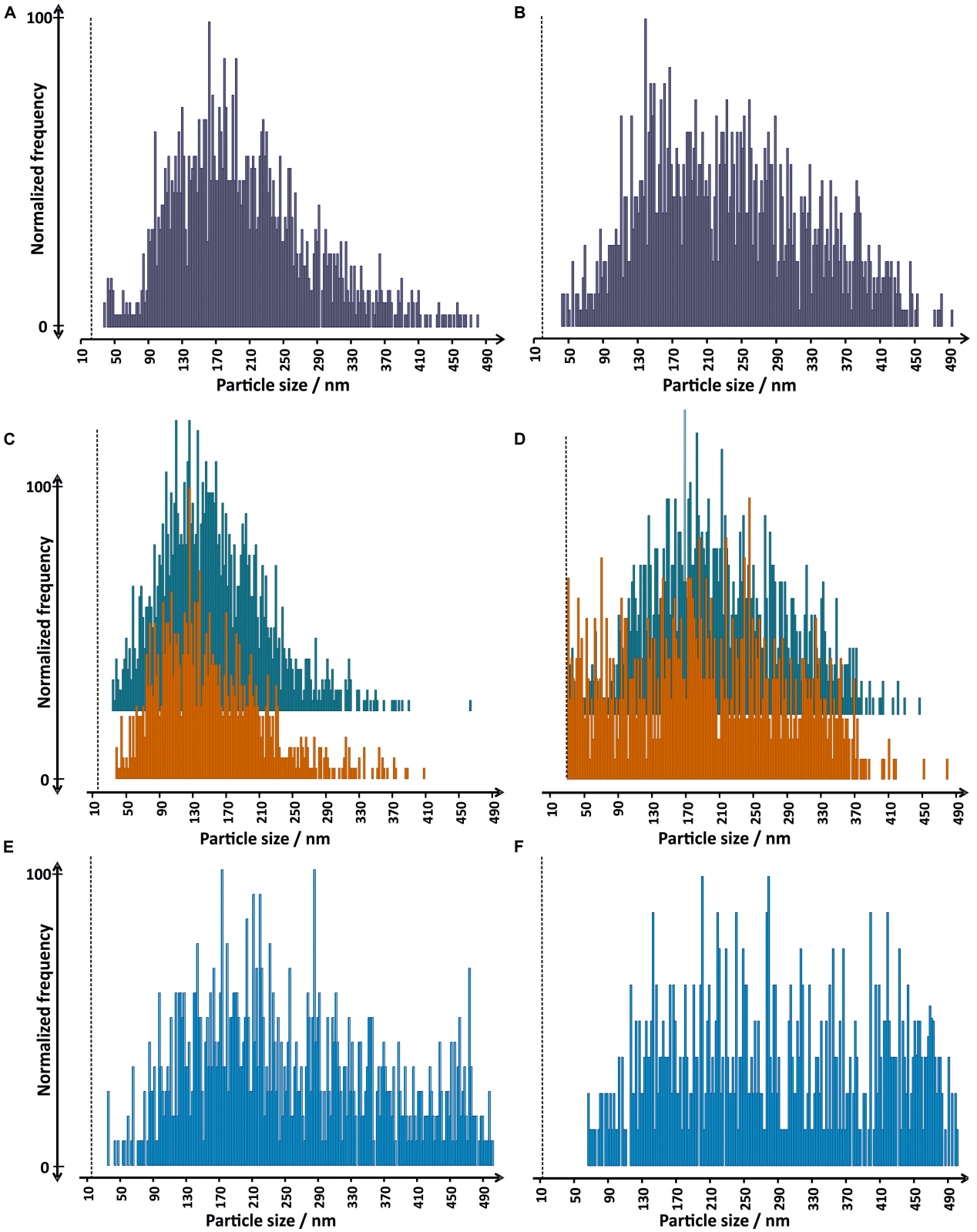

FIGURE 2 | Size distributions obtained by SP-ICP-MS for commercial TiO_2 NP suspensions in ultrapure water: **(A)** A and **(B)** B, used during plant cultivation; TiO_2 NP stock suspension **(C)** A, and **(D)** B, freshly prepared (blue) and after enzymatic digestion procedure (orange); and commercial suspensions **(E)** A and **(F)** B, after 7 days in contact with growth medium. Vertical lines represent the size limit of detection for each sample.

TABLE 2 | Median diameters, particle number concentrations, and mass concentrations obtained by SP-ICP-MS for the analysis of stock TiO_2 NP suspensions, the same nanoparticle suspensions after 7 days in contact with the growth medium, after enzymatic digestion procedure and extraction from plant tissues.

	Diameter/nm				
TiO_2 suspension	**Stock suspension**	**Enzymatic digestion**	**Growth medium**	**Leaves of treated plants**	**Roots of treated plants**
A	180 ± 13	188 ± 9	238 ± 13*	121 ± 1*	118 ± 5*
B	220 ± 10	215 ± 8	276 ± 12*	115 ± 2*	116 ± 2*
	Mass concentration/ng L^{-1}				
A	1745 ± 233	1241 ± 211	2419 ± 338	725 ± 49	751 ± 97
B	2556 ± 351	1507 ± 13	2671 ± 270	437 ± 12	539 ± 12
	Particle number concentration/NPs L^{-1}				
A	$6.51 \pm 0.61 \times 10^7$	$9.39 \pm 0.32 \times 10^7$	$3.40 \pm 0.53 \times 10^7$	$6.61 \pm 0.29 \times 10^7$	$7.50 \pm 0.32 \times 10^7$
B	$6.10 \pm 0.51 \times 10^7$	$4.84 \pm 0.45 \times 10^7$	$2.69 \pm 0.41 \times 10^7$	$4.15 \pm 0.10 \times 10^7$	$5.47 \pm 0.17 \times 10^7$

*All results are expressed as mean ± SD with n = 3. *Diameters presenting no significant differences with diameter obtained for stock suspension with a level of confidence >99% (one-way ANOVA).*

TABLE 3 | Comparison of median diameters, particle number concentrations, mass concentrations, and number of detected events obtained for two TiO_2 suspensions before and after filtration through a 0.45-μm pore size filter.

	Particle number concentration/NPs L^{-1}		Mass concentration/ng L^{-1}		Diameter/nm		Number or detected events	
TiO_2 suspension	**Before filtr.**	**After filtr.**	**Before filtr.**	**After filtr.**	**Before filtr.**	**After filtr.**	**Before filtr.**	**After filtr.**
A	$6.51 \pm 0.61 \times 10^7$	$9.97 \pm 0.42 \times 10^6$	1745 ± 233	80 ± 3	180 ± 13	129 ± 8	1445 ± 44	176 ± 35
B	$6.10 \pm 0.51 \times 10^7$	$2.08 \pm 0.30 \times 10^6$	2556 ± 351	20 ± 3	220 ± 10	157 ± 3	1299 ± 33	47 ± 11

All results are expressed as mean ± SD with n = 3.

reproducibility was observed, discarding any impact that this procedure may have on the determination of nanoparticle number concentration.

In conclusion, an analytical method based on monitoring ^{48}Ti by single-particle ICP-QQQ-MS followed by enzymatic digestion without filtration has been developed and optimized for the characterization and quantification of TiO_2 NPs in plant tissues.

Characterization of TiO_2 NPs in Radish

Investigation of TiO_2 NP Stability in the Growth Medium

First, the stability of TiO_2 NPs was tested in the growth media used for plant cultivation. TiO_2 NP suspensions of 5 mg L^{-1} were spiked into the nutrient solution, and the size distributions of the nanoparticles were determined by means of SP-ICP-MS after 7 days (**Figures 2E,F**). The results have shown the presence of several nanoparticles with bigger sizes (between 400 and 500 nm) than those obtained for the stock suspensions of both commercial TiO_2 NP suspensions. As a result, the median diameters obtained for both suspensions were shifted around 50 nm toward bigger sizes (**Table 2**) and hence presented significant differences with respect to stock solution (one-way ANOVA, level of confidence >99%). These results suggested that TiO_2 NPs undergo agglomeration to a small degree during the 7-day contact with the growth medium. On the other hand, no background signal corresponding to dissolved titanium was observed on the SP-ICP-MS time scans of both suspensions, showing that TiO_2 NPs did not undergo dissolution during the plant cultivation.

Single-Particle ICP-MS Analysis of Leaves Plus Stems and Roots of Radish

In order to study the uptake of TiO_2 NPs by radish, samples of roots and samples of leaves plus stems of plants treated with both nanoparticle suspensions were subjected to the enzymatic procedure followed by SP-ICP-MS analysis with the optimized conditions of H_2 and O_2 gas flows. Before the analysis of treated samples, roots and leaves plus stems of control plants were analyzed and the corresponding time scans obtained (**Figures 3A,B**). A few pulses above the background were observed for control plants. The occurrence of these pulses was not significant (less than 15 pulses out of 600,000 readings); in addition, a similar number of pulses (<15 particle events) were observed for the analysis of ultrapure water due to a carryover effect and did not have any effect on further analyses of treated plant tissues. On the other hand, low background signals were obtained for both tissues, and hence the possibility of having interference on titanium signal due to the plant matrix was discarded.

Afterward, radish tissues treated with both TiO_2 NP suspensions were analyzed by SP-ICP-MS, after enzymatic sample preparation procedure. Before SP-ICP-MS analysis, samples of leaves plus stems were diluted 100 times while samples of roots were diluted 5000 times, for TiO_2 NP suspension A. In the case of radish tissues treated with TiO_2 NP suspension B, samples were diluted 20 and 10000 times for leaves and roots, respectively. Time scans obtained showed a significant number of pulses in both plant tissues for both nanoparticle suspensions (**Figures 3C–F**), proving that radish is able to uptake TiO_2 NPs and transport them into the aerial part of the plant. Taking into

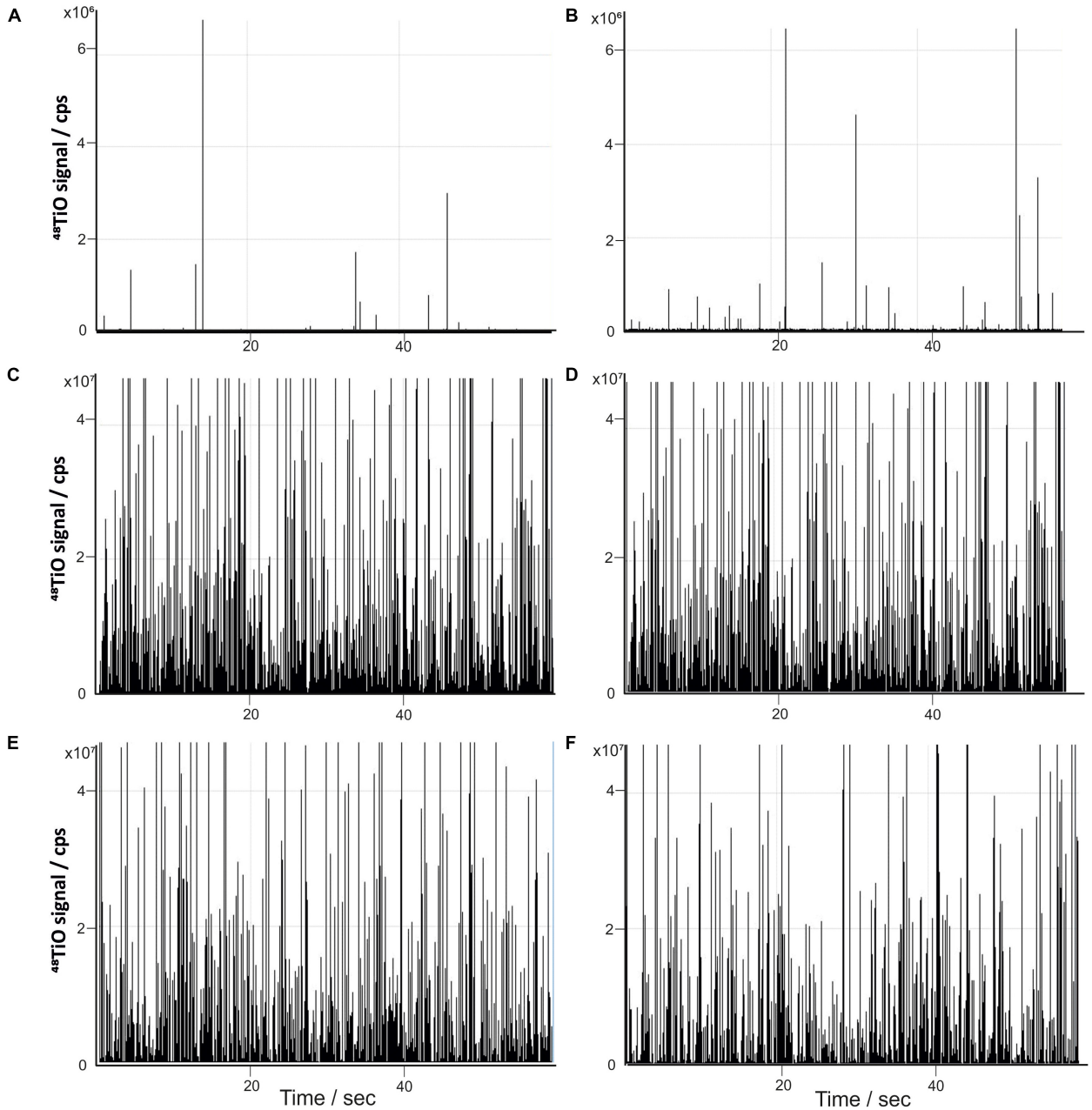

FIGURE 3 | Time scans obtained by SP-ICP-MS for **(A)** roots of control plants, **(B)** leaves plus stems of control plants, **(C)** roots of plants treated with TiO_2 NP suspension A, **(D)** leaves plus stems of plants treated with TiO_2 NP suspension A, **(E)** roots of plants treated with TiO_2 NP suspension B, and **(F)** leaves plus stems of plants treated with TiO_2 NP suspension B.

account the number of pulses detected, the nanoparticle number concentration in roots and in leaves together with stems was calculated as 3.7×10^{11} and 3.3×10^{9} NPs L^{-1}, respectively, for TiO_2 NP suspension A and as 5.5×10^{11} and 8.3×10^{8} NPs L^{-1} for suspension B.

Size distributions obtained from time scans for roots and leaves plus stems treated with both TiO_2 NP suspensions are shown on **Figure 4**. Although plant cells are surrounded by the cell wall that has pores with diameters ranging from 5 to 30 nm (Tan et al., 2018) and in theory only small TiO_2 NPs are likely to enter plants through cell wall pores, the presence of particles above 100 nm was detected in both radish tissues. It could indicate that TiO_2 NPs possibly enlarged cell pores or created new ones, as it has been suggested (Tan et al., 2018). Remarkably, the size distributions of nanoparticles from both suspensions extracted from roots did not show the presence of bigger nanoparticles and/or agglomerates (**Figures 4A,B**), presenting median diameters smaller than those

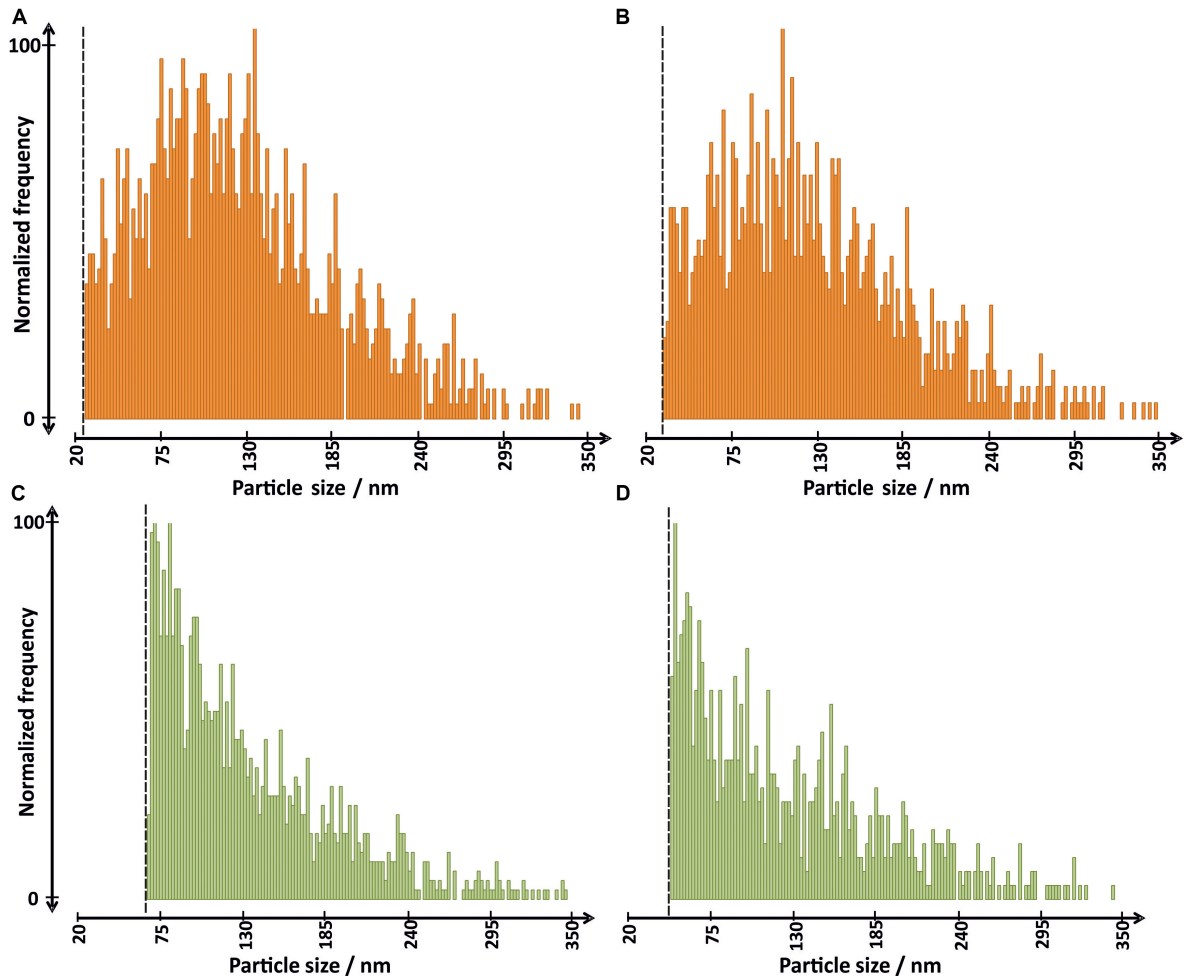

FIGURE 4 | Size distributions obtained by SP-ICP-MS for **(A)** roots of plants treated with TiO_2 NP suspension A, **(C)** leaves plus stems of plants treated with TiO_2 NP suspension A, **(B)** roots of plants treated with TiO_2 NP suspension B, and **(D)** leaves plus stems of plants treated with TiO_2 NP suspension B. Vertical lines represent the size limit of detection for each sample.

of the distributions obtained for fresh suspensions (**Table 2**), suggesting a preferential uptake of smaller nanoparticles and the occurrence of some redispersion. A similar behavior has been observed for other metal and metal-oxide nanoparticles (Kińska et al., 2018; Wojcieszek et al., 2019). On the other hand, one-way ANOVA revealed no significant differences, with a level of confidence of >99%, between nanoparticle diameters obtained for leaves and roots of plants treated with both TiO_2 NP suspensions (**Table 2**). From the results obtained, it can be concluded that nanoparticles did not undergo agglomeration during their translocation to aboveground tissues. It should also be highlighted that the use of a $5\sigma_b$ criterion to discriminate between nanoparticle events and dissolved signal may lead to the occurrence of false negatives, i.e., small nanoparticles below the size limit of detection are considered as background and hence not reflected in the corresponding size distribution. This fact is especially important for the size distribution obtained for nanoparticles in leaves (**Figures 4C,D**) where the presence of a higher background signal implied a higher size limit of detection (reported in **Figure 4** as a vertical line), which leads to the apparent loss of small nanoparticles in the histogram. Although smaller nanoparticles could not be detected, the occurrence of a redispersion process in leaf tissues should not be ignored, as it was shown for samples after enzymatic digestion and root samples.

Unlike other metal-oxide NPs, including CuO, ZnO, or even CeO_2 NPs, TiO_2 NPs have very high stability and low dissolution rate (Schmidt and Vogelsberger, 2006; Tan et al., 2018). Moreover, the root-to-shoot translocation factor was found to be low, although results have proved that TiO_2 NPs can be transported from roots to aboveground tissues. Previous studies by using various analytical techniques have already reported the presence of TiO_2 NPs in different plants such as barley, thale cress, or wheat, showing accumulation of NPs mainly in roots (Kurepa et al., 2010; Mattiello et al., 2015; Jiang et al., 2017). Finally, SP-ICP-MS (with a single-quadrupole instrument) and electron microscopy were used in order to study the translocation of TiO_2 NPs in rice (*Oryza sativa* L.), showing the presence of NPs in both roots and aboveground organs

(Deng et al., 2017). However, only the less abundant isotope of Ti (^{49}Ti) was monitored. In the case of the present study, the not engagement of a collision cell would have resulted in a significant number of nanoparticles missed in roots and leaf samples.

CONCLUSION

The using of a triple-quadrupole ICP operating in tandem mass spectrometry and single-particle mode (SP-ICP-QQQ-MS) allowed the reduction in the background signal in plant matrices for monitoring the most sensitive isotope of titanium. Under the optimal conditions of reaction cells, the uptake, translocation, and transformations of two TiO_2 NPs with different nominal sizes in radish were investigated by single-particle ICP-MS for the first time. The results demonstrated that both types of TiO_2 NPs underwent agglomeration in a small degree after 7 days in contact with the growth medium, but the enzymatic digestion procedure performed for their extraction from plant tissues did not affect the integrity of the studied nanoparticles. On the other hand, the use of filtration after the enzymatic treatment was discarded, due to the loss of the majority of nanoparticles because of membrane adsorption. The analysis of roots indicated that radish only takes up smaller nanoparticles since the presence of bigger nanoparticles was not observed for both TiO_2 NP suspensions studied. Additionally, the presence of nanoparticles without significant changes in diameter was observed in both leaves and roots, proving the plant's ability to translocate TiO_2 NPs up to aboveground organs without undergoing any transformation like dissolution or agglomeration. Finally, it should be noted that the uptake of TiO_2 NPs by plants may be favored by hydroponic cultivation, which may induce root damage allowing the nanoparticles to pass the Casparian strip and later be transported to leaves via the xylem. In this context, studies about the uptake of nanoparticles by plants in soil and at lower nanoparticle concentrations are needed.

DATA AVAILABILITY STATEMENT

The raw data supporting the conclusions of this article will be made available by the authors, without undue reservation.

AUTHOR CONTRIBUTIONS

JW and JJ-L wrote the manuscript. JW performed the single-particle ICP-MS analysis experiments. MA performed the plant cultivations. JW, JJ-L, LR, MJ, and JS conceived the project, designed the experiments, and interpreted the results. LR and JS corrected and improved the manuscript. MJ financed the research. All authors contributed to the article and approved the submitted version.

FUNDING

This work was financially supported by the National Science Centre, Poland (grant No. 2015/18/M/ST4/00257) and Warsaw University of Technology.

ACKNOWLEDGMENTS

The authors would like to thank Maciej Trzaskowski [Centre for Advanced Materials and Technologies (CEZAMAT), Warsaw University of Technology], for SEM analysis of TiO_2 NPs suspensions.

SUPPLEMENTARY MATERIAL

The Supplementary Material for this article can be found online at: https://www.frontiersin.org/articles/10.3389/fenvs.2020.00100/full#supplementary-material

REFERENCES

Azimzada, A., Farner, J. M., Hadioui, M., Liu-Kang, C., Jreije, I., Tufenkji, N., et al. (2020). Release of TiO2 nanoparticles from painted surfaces in cold climates: characterization using a high sensitivity single-particle ICP-MS. *Environ. Sci. Nano* 7, 139–148. doi: 10.1039/c9en00951e

Burke, D. J., Pietrasiak, N., Situ, S. F., Abenojar, E. C., Porche, M., Kraj, P., et al. (2015). Iron oxide and titanium dioxide nanoparticle effects on plant performance and root associated microbes. *Int. J. Mol. Sci.* 16, 23630–23650. doi: 10.3390/ijms161023630

Cai, F., Wu, X., Zhang, H., Shen, X., Zhang, M., Chen, W., et al. (2017). Impact of TiO2 nanoparticles on lead uptake and bioaccumulation in rice (*Oryza sativa* L.). *NanoImpact* 5, 101–108. doi: 10.1016/j.impact.2017.01.006

Capaldi Arruda, S. C., Diniz Silva, A. L., Moretto Galazzi, R., Antunes Azevedo, R., and Zezzi Arruda, M. A. (2015). Nanoparticles applied to plant science: a review. *Talanta* 131, 693–705. doi: 10.1016/j.talanta.2014.08.050

Castillo-Michel, H. A., Larue, C., Pradas del Real, A. E., Cotte, M., and Sarret, G. (2017). Practical review on the use of synchrotron based micro- and nano-X-ray fluorescence mapping and X-ray absorption spectroscopy to investigate the interactions between plants and engineered nanomaterials. *Plant Physiol. Biochem.* 110, 13–32. doi: 10.1016/j.plaphy.2016.07.018

Chen, X., and Mao, S. S. (2007). Titanium dioxide nanomaterials: synthesis, properties, modifications and applications. *Chem. Rev.* 107, 2891–2959. doi: 10.1021/cr0500535

Dan, Y., Zhang, W., Xue, R., Ma, X., Stephan, C., Shi, H. (2015). Characterization of gold nanoparticle uptake by tomato plants using enzymatic extraction followed by single-particle inductively coupled plasma-mass spectrometry analysis. *Environ. Sci. Technol.* 49, 3007–3014. doi: 10.1021/es506179e

Dar, G. I., Saeed, M., and Wu, A. (2020). "Toxicity of TiO_2 nanoparticles," in *TiO_2 Nanoparticles: Applications in Nanobiotechnology and Nanomedicine*. doi: 10.1002/9783527825431.ch2

Deng, Y., Petersen, E. J., Challis, K. E., Rabb, S. A., Holbrook, R. D., Ranville, J. F., et al. (2017). Multiple Method Analysis of TiO2 Nanoparticle Uptake in Rice (*Oryza sativa* L.) Plants. *Environ. Sci. Technol.* 51, 10615–10623. doi: 10.1021/acs.est.7b01364

Du, J., Xu, S., Zhou, Q., Li, H., Fu, L., Tang, J. H., et al. (2019). The ecotoxicology of titanium dioxide nanoparticles, an important engineering nanomaterial. *Toxicol. Environ. Chem.* 101, 165–189. doi: 10.1080/02772248.2019.1693572

Du, W., Gardea-Torresdey, J. L., Xie, Y., Yin, Y., Zhu, J., Zhang, X., et al. (2017). Elevated CO2 levels modify TiO2 nanoparticle effects on rice and soil microbial

communities. *Sci. Total Environ.* 578, 408–416. doi: 10.1016/j.scitotenv.2016.10.197

Fedotov, P. S., Vanifatova, N. G., Shkinev, V. M., and Spivakov, B. Y. (2011). Fractionation and characterization of nano- and microparticles in liquid media. *Anal. Bioanal. Chem.* 400, 1787–1804. doi: 10.1007/s00216-011-4704-1

Hadioui, M., Knapp, G., Azimzada, A., Jreije, I., Frechette-Viens, L., Wilkinson, K. J. (2019). Lowering the size detection limits of Ag and TiO2 nanoparticles by single particle ICP-MS. *Anal. Chem.* 91, 13275–13284. doi: 10.1021/acs.analchem.9b04007

Hong, F., Yu, X., Wu, N., and Zhang, Y. Q. (2017). Progress of: in vivo studies on the systemic toxicities induced by titanium dioxide nanoparticles. *Toxicol. Res.* 6, 115–133. doi: 10.1039/c6tx00338a

Jafarizadeh-Malmiri, H., Sayyar, Z., Anarjan, N., and Berenjian, A. (2019). *Nanobiotechnology in Food: Concepts, Applications and Perspectives*. 1–155. doi: 10.1007/978-3-030-05846-3

Jiang, F., Shen, Y., Ma, C., Zhang, X., Cao, W., Rui, Y. (2017). Effects of TiO2 nanoparticles on wheat (*Triticum aestivum* L.) seedlings cultivated under super-elevated and normal CO2 conditions. *PLoS One* 12:e178088. doi: 10.1371/journal.pone.0178088

Jiménez-Lamana, J., Wojcieszek, J., Jakubiak, M., Asztemborska, M., and Szpunar, J. (2016). Single particle ICP-MS characterization of platinum nanoparticles uptake and bioaccumulation by Lepidium sativum and Sinapis alba plants. *J. Anal. At. Spectrom.* 31, 2321–2329. doi: 10.1039/C6JA00201C

Keller, A. A., and Lazareva, A. (2013). Predicted releases of engineered nanomaterials: from global to regional to local. *Environ. Sci. Technol. Lett.* 1, 65–70. doi: 10.1021/ez400106t

Kińska, K., Jiménez-Lamana, J., Kowalska, J., Krasnodębska-Ostręga, B., and Szpunar, J. (2018). Study of the uptake and bioaccumulation of palladium nanoparticles by Sinapis alba using single particle ICP-MS. *Sci. Total Environ.* 615, 1078–1085. doi: 10.1016/j.scitotenv.2017.09.203

Kole, C., Kumar, D. S., and Khodakovskaya, M. V. (2016). Biophysical methods of detection and quantification of uptake, translocation, and accumulation of nanoparticles. *Plant Nanotechnol.* 29–63. doi: 10.1007/978-3-319-42154-4

Kurepa, J., Paunesku, T., Vogt, S., Arora, H., Rabatic, B. M., Lu, J., et al. (2010). Uptake and distribution of ultrasmall anatase TiO2 alizarin red s nanoconjugates in arabidopsis thaliana. *Nano Lett.* 10, 2296–2302. doi: 10.1021/nl903518f

Laborda, F., Bolea, E., and Jiménez-Lamana, J. (2014). Single particle inductively coupled plasma mass spectrometry: a powerful tool for nanoanalysis. *Anal. Chem.* 86, 2270–2278. doi: 10.1021/ac402980q

Laborda, F., Bolea, E., and Jiménez-Lamana, J. (2016). Single particle inductively coupled plasma mass spectrometry for the analysis of inorganic engineered nanoparticles in environmental samples. *Trends Environ. Anal. Chem.* 9, 15–23. doi: 10.1016/j.teac.2016.02.001

Laborda, F., Gimenez-Ingalaturre, A. C., Bolea, E., and Castillo, J. R. (2019). Single particle inductively coupled plasma mass spectrometry as screening tool for detection of particles. *Spectrochim. Acta Part B At. Spectrosc.* 159:105654. doi: 10.1016/j.sab.2019.105654

Larue, C., Castillo-Michel, H., Sobanska, S., Trcera, N., Sorieul, S., Cécillon, L., et al. (2014). Fate of pristine TiO2 nanoparticles and aged paint-containing TiO2 nanoparticles in lettuce crop after foliar exposure. *J. Hazard. Mater.* 273, 17–26. doi: 10.1016/j.jhazmat.2014.03.014

Larue, C., Castillo-Michel, H., Stein, R. J., Fayard, B., Pouyet, E., Villanova, J., et al. (2016). Innovative combination of spectroscopic techniques to reveal nanoparticle fate in a crop plant. *Spectrochim. Acta Part B At. Spectrosc.* 119, 17–24. doi: 10.1016/j.sab.2016.03.005

Lee, S., Bi, X., Reed, R. B., Ranville, J. F., Herckes, P., Westerhoff, P. (2014). Nanoparticle size detection limits by single particle ICP-MS for 40 elements. *Environ. Sci. Technol.* 48, 10291–10300. doi: 10.1021/es502422v

Mattiello, A., Filippi, A., Pošćić, F., Musetti, R., Salvatici, M. C., Giordano, C., et al. (2015). Evidence of phytotoxicity and genotoxicity in *Hordeum vulgare* L. Exposed to CeO2 and TiO2 Nanoparticles. *Front. Plant Sci.* 6:1043. doi: 10.3389/fpls.2015.01043

Oliver, A. L. S., Muñoz-Olivas, R., Sanz Landaluze, J., Rainieri, S., and Cámara, C. (2015). Bioaccumulation of ionic titanium and titanium dioxide nanoparticles in zebrafish eleutheroembryos. *Nanotoxicology* 9, 835–842. doi: 10.3109/17435390.2014.980758

Pace, H. E., Rogers, N. J., Jarolimek, C., Coleman, V. A., Higgins, C. P., Ranville, J. F., et al. (2011). Determining transport efficiency for the purpose of counting and sizing nanoparticles via single particle inductively coupled plasma mass spectrometry. *Anal. Chem.* 83, 9361–9369. doi: 10.1021/ac201952t

Reddy, P. V. L., Hernandez-Viezcas, J. A., Peralta-Videa, J. R., and Gardea-Torresdey, J. L. (2016). Lessons learned: are engineered nanomaterials toxic to terrestrial plants? *Sci. Total Environ.* 568, 470–479. doi: 10.1016/j.scitotenv.2016.06.042

Schmidt, J., and Vogelsberger, W. (2006). Dissolution kinetics of titanium dioxide nanoparticles: the observation of an unusual kinetic size effect. *J. Phys. Chem. B* 110, 3955–3963. doi: 10.1021/jp055361l

Servin, A. D., Castillo-Michel, H., Hernandez-Viezcas, J. A., Diaz, B. C., Peralta-Videa, J. R., Gardea-Torresdey, J. L., et al. (2012). Synchrotron micro-XRF and micro-XANES confirmation of the uptake and translocation of TiO2 nanoparticles in cucumber (*Cucumis sativus*) plants. *Environ. Sci. Technol.* 46, 7637–7643. doi: 10.1021/es300955b

Servin, A. D., Morales, M. I., Castillo-Michel, H., Hernandez-Viezcas, J. A., Munoz, B., Zhao, L., et al. (2013). Synchrotron verification of TiO2 accumulation in cucumber fruit: a possible pathway of TiO2 nanoparticle transfer from soil into the food chain. *Environ. Sci. Technol.* 47, 11592–11598. doi: 10.1021/es403368j

Shah, S. N. A., Shah, Z., Hussain, M., and Khan, M. (2017). Hazardous effects of titanium dioxide nanoparticles in ecosystem. *Bioinorg. Chem. Appl.* 2017:4101735. doi: 10.1155/2017/4101735

Shakeel, M., Jabeen, F., Shabbir, S., Asghar, M. S., Khan, M. S., Chaudhry, A. S., et al. (2016). Toxicity of Nano-Titanium Dioxide (TiO2-NP) through various routes of exposure: a review. *Biol. Trace Elem. Res.* 172, 1–36. doi: 10.1007/s12011-015-0550-x

Tan, W., Peralta-Videa, J. R., and Gardea-Torresdey, J. L. (2018). Interaction of titanium dioxide nanoparticles with soil components and plants: current knowledge and future research needs-a critical review. *Environ. Sci. Nano* 5, 257–278. doi: 10.1039/c7en00985b

Tharaud, M., Gondikas, A. P., Benedetti, M. F., von der Kammer, F., Hofmann, T., Cornelis, G., et al. (2017). TiO2 nanomaterial detection in calcium rich matrices matrices by spICPMS . A matter of resolution and treatment. *J. Anal. At. Spectrom.* 32, 1400–1411. doi: 10.1039/C7JA00060J

Thor, K. (2019). Calcium — nutrient and messenger. *Front. Plant Sci.* 10:440. doi: 10.3389/fpls.2019.00440

Vidmar, J., Milačič, R., and Ščančar, J. (2017). Sizing and simultaneous quantification of nanoscale titanium dioxide and a dissolved titanium form by single particle inductively coupled plasma mass spectrometry. *Microchem. J.* 132, 391–400. doi: 10.1016/j.microc.2017.02.030

White, P. J., and Broadley, M. R. (2003). Calcium in plants. *Ann. Bot.* 92, 487–511. doi: 10.1093/aob/mcg164

Wojcieszek, J., Jiménez-Lamana, J., Bierła, K., Ruzik, L., Asztemborska, M., Jarosz, M., et al. (2019). Uptake, translocation, size characterization and localization of cerium oxide nanoparticles in radish (*Raphanus sativus* L.). *Sci. Total Environ.* 683, 284–292. doi: 10.1016/j.scitotenv.2019.05.265

Zahra, Z., Waseem, N., Zahra, R., Lee, H., Badshah, M. A., Mehmood, A., et al. (2017). Growth and Metabolic Responses of Rice (*Oryza sativa* L.) Cultivated in Phosphorus-Deficient Soil Amended with TiO2 Nanoparticles. *J. Agric. Food Chem.* 65, 5598–5606. doi: 10.1021/acs.jafc.7b01843

Zhang, X., Li, W., and Yang, Z. (2015). Toxicology of nanosized titanium dioxide: an update. *Arch. Toxicol.* 89, 2207–2217. doi: 10.1007/s00204-015-1594-6

Conflict of Interest: The authors declare that the research was conducted in the absence of any commercial or financial relationships that could be construed as a potential conflict of interest.